Bacterial chemotaxis and the question of gain

Receptor sensitivity in bacterial chemotaxis

Victor Sourjik and Howard C. Berg*

Department of Molecular and Cellular Biology, Harvard University, Cambridge, MA 02138; and Rowland Institute for Science, Cambridge, MA 02142

Contributed by Howard C. Berg, November 2, 2001

Chemoreceptors in *Escherichia coli* are coupled to the flagella by a labile phosphorylated intermediate, CheY~P. Its activity can be inferred from the rotational bias of flagellar motors, but motor response is stochastic and limited to a narrow physiological range. Here we use fluorescence resonance energy transfer to monitor interactions of CheY~P with its phosphatase, CheZ, that reveal changes in the activity of the receptor kinase, CheA, resulting from the addition of attractants or repellents. Analyses of *cheR* and/or *cheB* mutants, defective in receptor methylation/demethylation, show that response sensitivity depends on the activity of CheB and the level of receptor modification. In *cheRcheB* mutants, the concentration of attractant that generates a half-maximal response is equal to the dissociation constant of the receptor. In wild-type cells, it is 35 times smaller. This amplification, together with the ultrasensitivity of the flagellar motor, explains previous observations of high chemotactic gain.

Escherichia coli | fluorescence | fluorescence resonance energy transfer

Bacteria move up spatial gradients of chemical attractants in a biased random walk, now running smoothly, now tumbling randomly, extending runs that carry them in a favorable direction (1). The central point of regulation in the chemotaxis signal transduction pathway is the level of phosphorylation of the diffusible signaling protein CheY (2). CheY is phosphorylated by the kinase CheA that is coupled to specific receptors (3). CheY~P binds to FliM, a component of the switch complex, at the cytoplasmic face of the flagellar motor and modulates the direction of motor rotation (4–6). The phosphatase CheZ binds to CheY~P and accelerates its dephosphorylation (7, 8). The receptor is thought to exist in two states, active (activating CheA) and inactive (inhibiting CheA) (9). Attractant binding lowers the probability of the active state, decreasing the level of CheY~P. Attractant removal raises the probability of the active state, increasing the level of CheY~P. Adaptation is by receptor methylation by CheR and demethylation by CheB (10–12). Receptor methylation compensates for attractant binding, with the modified receptor more likely to be in the active state. Thus, CheR promotes adaptation to increasing levels of attractants, and CheB promotes adaptation to decreasing levels of attractants. Two major chemoreceptors exist in *Escherichia coli*: the aspartate receptor, Tar, and serine receptor, Tsr. Tar has four methylation sites, which are glutamates; however, two of these are expressed as glutamines, deamidated by CheB. The glutamines are thought to be physiologically equivalent to methylated glutamates (13).

We used fluorescence resonance energy transfer (FRET) to measure intracellular changes in phosphorylation-dependent interactions of CheY upon chemotactic stimulation. FRET, which relies on the distance-dependent transfer of energy from an excited donor fluorophore to an acceptor fluorophore, is one of the few tools available for monitoring protein interactions in real time *in vivo* (14–17). It is particularly useful, as in the present case, when components are labile; in a cell containing CheZ, the half-life of CheY~P is only a few tenths of a second. We made a yellow fluorescent protein (YFP) fusion to CheY (CheY-YFP) as acceptor and a cyan fluorescent protein (CFP) fusion to CheZ (CheZ-CFP) as donor, adsorbed cells containing fusion pairs to the coverslip of a flow cell, and measured changes in the ratio of yellow to cyan emission after addition or removal of attractants or repellents.

Our main result is the discovery of large sensitivity amplification at the beginning of the signal transduction pathway. The fractional change in kinase activity is about 35 times larger than the fractional change in receptor occupancy. When combined with the ultrasensitivity of the flagellar motor demonstrated by Cluzel *et al.* (18), this amplification explains the long-standing paradox of high chemotactic gain (19).

Materials and Methods

Bacterial Strains. Fusions to CheY and CheZ of YFP and CFP (CLONTECH) were made as described (20). The *cheY-eyfp* fusion was cloned into pTrc99A (Amp^R; Amersham Pharmacia) under an isopropyl β-D-thiogalactoside-inducible promoter, yielding pVS18. The *cheZ-ecfp* fusion was cloned into pBAD33 (Cm^R) under an arabinose-inducible promoter (21), yielding pVS54. In the background strains used here, this promoter allows gradual induction of gene expression (20). These strains, derived from RP437 or RP2893 [Δ*2206*(*tap-cheZ*)], were made by the methods described (20): VS104 [Δ(*cheY-cheZ*), referred to as wildtype], VS127 [Δ*cheR* Δ(*cheY-cheZ*)], VS131 [Δ*2206*(*tap-cheZ*) *tarQ309E*], VS134 [Δ*2206*(*tap-cheZ*) *tar*(*Q295E Q309E*)], VS147 [Δ*2206(tap-cheZ*) *tarE491Q*], VS124 [Δ(*cheB-cheZ*)], and VS135 [Δ(*cheB-cheZ*) *tar*(*Q295E Q309E*)].

Preparation of Cells. Cells containing the CheY/CheZ constructs pVS18/pVS54 were grown as described (20) in the presence of 100 μg/ml ampicillin, 34 μg/ml chloramphenicol, 0.05 mM isopropyl β-D-thiogalactoside, and 100 μg/ml arabinose. These induction levels were chosen to give optimal complementation in *cheYcheZ* mutants. Cells were collected by centrifugation (5 min at 5,000 × *g*) and washed twice with tethering buffer (10 mM KPO_4/0.1 mM EDTA/1 μM methionine/10 mM lactic acid, pH 7). Cells were attached to a polylysine-coated coverslip (20) and placed in the flow cell (22). The flow cell was kept under constant flow (tethering medium at 1 ml/min) by a syringe pump (Harvard Apparatus 22). The same flow was used to add and remove attractants (α-methyl-DL-aspartate, Sigma M-6001; synthetic L-aspartate, ICN 100809) or repellent ($NiCl_2$, Fisher N-54). With this flow rate and 0.5 μM fluorescein as a marker, the time required to achieve 90% and 99% replacement was <4 sec and <6 sec, respectively. Removal of 99% of the fluorescein took <12 sec, but some delay might have occurred from adsorption to polylysine.

Data Acquisition. The measurements were made with an upright microscope (Nikon Optiphot) equipped with two epifluorescence attachments mounted in tandem, which allowed light from the objective (Nikon Plan Fluor 40×) to be analyzed by two fluorescence cubes (both by Chroma Technology, Brattleboro,

Abbreviations: FRET, fluorescence resonance energy transfer; YFP, yellow fluorescent protein; CFP, cyan fluorescent protein; MeAsp, α-methylaspartate.

See commentary on page 7.

*To whom reprint requests should be addressed. E-mail: hberg@biosun.harvard.edu.

The publication costs of this article were defrayed in part by page charge payment. This article must therefore be hereby marked "*advertisement*" in accordance with 18 U.S.C. §1734 solely to indicate this fact.

VT). Light passing through the dichroic mirror of the lower cube (455DC) was split at the upper cube by a second dichroic mirror (515DC) and passed through two emission filters, one yellow-green (HQ535/30), positioned at the top of the upper fluorescence attachment, and the other blue-green (D485/40), positioned at the back of the upper fluorescence attachment. We call these two beams yellow and cyan, because they monitor the emission of the yellow and cyan fluorescent proteins, respectively; however, some of the light emitted by CFP is transmitted by the yellow-green filter. Excitation was by a He-Cd laser (442 nm, 15 mW, Melles Griot 4056R-S-A01, Irvine CA). The system was designed so that evanescent-wave excitation could be used (23), but standard epifluorescence proved simpler. In the latter mode, the laser light was attenuated by a factor of 400 with neutral-density filters, passed by a blue excitation filter (D440/20) and reflected downward by the dichroic mirror in the lower fluorescence cube. A spot about 100 μm in diameter illuminated the object plane. The emitted light was detected by photon-counting photomultipliers (Hamamatsu H7421–40, Hamamatsu, Bridgewater, NJ) whose outputs were converted to analog signals by ratemeters (RIS-375, Rowland Institute), filtered by 8-pole low-pass Bessel filters (2-Hz cutoff frequency, Krohn-Hite 3384, Krohn-Hite, Avon, MA) and sampled at 5 Hz by a computer data-acquisition system (National Instruments LABVIEW 5.1 and Macintosh G3).

Data Analysis. We assume that the yellow and cyan fusion proteins are either dissociated or associated. When they are dissociated, the light intensities in the yellow and cyan channels are Y0 and C0, respectively, and their ratio is $Y0/C0 = R0$. The changes in intensities observed when one pair of yellow and cyan fusion proteins associate are ΔY and ΔC, respectively. When N pairs associate, these changes are $N\Delta Y$ and $N\Delta C$, respectively. Therefore, the final intensities are $Y0 + N\Delta Y$ and $C0 + N\Delta C$, and their ratio is $R = (Y0 + N\Delta Y)/(C0 + N\Delta C)$. Because ΔY is positive and ΔC is negative, R is larger than $R0$. Taking the difference of these ratios, $R - R0$, and solving for N, we find $N = (R - R0)(C0/\Delta C)/[(\Delta Y/\Delta C) - R]$. Because we measure $N\Delta Y$ and $N\Delta C$, we also know $N\Delta Y/N\Delta C = \Delta Y/\Delta C$. So the only parameter in this equation that is not determined is ΔC. However, our interest is in the change in energy transfer upon chemotactic stimulation, so we can normalize N to the prestimulus value, N_{pre}, and determine the ratio $N/N_{pre} = \{(R - R0)/[(\Delta Y/\Delta C) - R]\}/\{(R_{pre} - R0)/[(\Delta Y/\Delta C) - R_{pre}]\}$. Here, R_{pre} is the yellow-to-cyan ratio observed in buffer before the addition of attractant or repellent, and R is the corresponding ratio measured after its addition. $R0$ is this ratio in the absence of energy transfer, which we simulate by addition of a saturating amount of attractant. The increase in cyan emission observed upon this addition was matched by an increase induced by bleaching of YFP, effected by exposure to light from a 532-nm diode laser (24), confirming that the saturating stimulus reduces CheY~P levels to negligible values. All the essential parameters are determined in each experiment. Changes in amplitudes of Y and C were ≈10–15%, resulting in changes of R of ≈20%. The intensity of the excitation light was so low that photobleaching reduced the values of Y and C by <0.5%/min and that of R by <0.2%/min. We monitored fluorescence from a field of 300–500 cells in each experiment and repeated each experiment at least three times by using different cell cultures. Figs. 2 and 3*A* show means and standard deviations. The data were fit to a multisite Hill model (25). For example, for a shift in the concentration of attractant from 0 to A, $1 - N/N_{pre} = A^H/(A^H + K_D{}^H)$, where K_D is the apparent dissociation constant (the value of A for half-maximal response), and H is the Hill coefficient. Because H proved to be small (≈1.2), a single-site model could have been used instead.

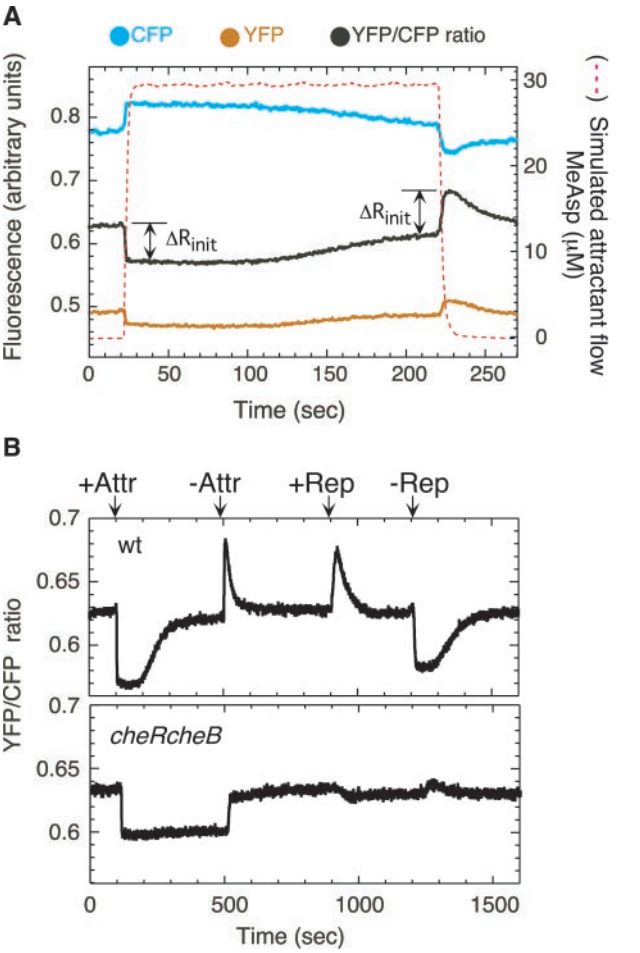

Fig. 1. Changes in protein–protein interactions observed by FRET upon chemotactic stimulation of cells of *E. coli* adsorbed to a coverslip. (*A*) Experimental scenario. Cells containing CheY/CheZ pairs were stimulated by stepwise addition or removal of attractant, MeAsp, as indicated by the dashed line (simulated by the flow of 0.5 μM fluorescein). Changes in protein–protein interactions result in changes in the ratio of fluorescence intensities of YFP and CFP. ΔR_{init} is the initial response to addition or removal of attractant. (*B*) FRET responses to addition/removal of attractant and to addition/removal of repellent for wild-type (wt) and mutant cells (*cheRcheB*) defective for methylation/demethylation. Stimulation levels were chosen to cause a near-saturating response. Attractant (Attr): 30 μM MeAsp for wt, 1.5 mM for *cheRcheB*. Repellent (Rep): 100 μM $NiCl_2$.

Results

In a typical experiment, α-methylaspartate (MeAsp), a nonmetabolizable aspartate analog, was added or removed stepwise by flow (Fig. 1*A*). A higher ratio of yellow to cyan emission indicates more energy transfer as a result of a larger number of interacting YFP/CFP pairs, that in turn indicates higher levels of CheY~P. Response of the same cell population to repeated addition or removal of different amounts of attractant could be tested, greatly reducing the errors associated with culture-to-culture variation. Changes in the CheY/CheZ interaction upon chemotactic stimulation reflected expected changes in the level of CheY~P (Fig. 1*B*). The initial response was followed by CheR/CheB-dependent adaptation, and response to repellent was opposite of that to attractant. The *cheRcheB* mutant showed reduced sensitivity and failed to adapt. It also failed to respond to repellent. No changes in the YFP/CFP fluorescence ratio were observed in response to chemotactic stimulation of strains expressing fusion protein pairs but no other chemotaxis or flagellar proteins (e.g., *flhC* strains; data not shown).

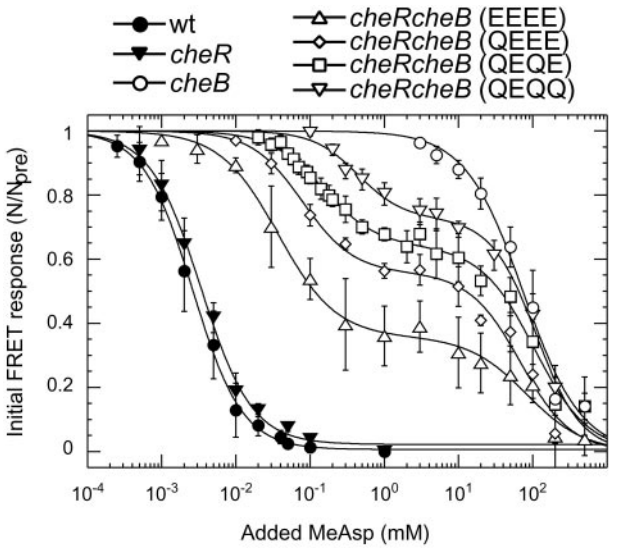

Fig. 2. Response of wild-type and *cheR* and/or *cheB* cells to steps of MeAsp at 0 ambient, measured with the CheY/CheZ FRET pair. Here, N/N_{pre} is the number of FRET pairs after the stimulus divided by the number of FRET pairs before the stimulus, with $N = 0$ determined by the addition of a saturating amount of attractant and verified by acceptor bleaching. MeAsp was added and then removed in a sequence of steps of increasing size. Modification states of genetically engineered Tar receptors are noted in parentheses: E, glutamate, and Q, glutamine. For *cheR* the modification state should be all E, for *cheRcheB* with the native receptor QEQE (as shown), and for *cheB* either half glutamines and half methylated glutamates or all methylated glutamates. The smooth curves are fits to the data of a multisite Hill model; *cheRcheB strains* have two K_D values, K_{D1} and K_{D2}, with β the amplitude of the response corresponding to K_{D1} and $(1 - \beta)$ the amplitude of the response corresponding to K_{D2}. For the wild type, $K_D = 2.6 \pm 0.5$ μM; for *cheR*, $K_D = 3.3 \pm 0.5$ μM; for *cheRcheB* (EEEE), $\beta = 0.65 \pm 0.02$, $K_{D1} = 38 \pm 5$ μM, $K_{D2} = 83 \pm 17$ mM; for *cheRcheB* (QEEE), $\beta = 0.46 \pm 0.02$, $K_{D1} = 80 \pm 15$ μM, $K_{D2} = 77 \pm 10$ mM; for *cheRcheB* (QEQE), $\beta = 0.36 \pm 0.02$, $K_{D1} = 150 \pm 15$ μM, $K_{D2} = 105 \pm 19$ mM; for *cheRcheB* (QEQQ), $\beta = 0.27 \pm 0.02$, $K_{D1} = 440 \pm 70$ μM, $K_{D2} = 110 \pm 10$ mM; and for *cheB*, $K_D = 75 \pm 18$ mM. Hill coefficients were 1.2 ± 0.1. The absolute sizes of the response amplitudes generated by addition of saturating amounts of MeAsp varied among wild type, *cheR*, *cheRcheB* (EEEE), *cheRcheB* (QEEE), *cheRcheB* (QEQE), *cheRcheB* (QEQQ), and *cheB* strains in the ratios 1:0.06:1.3:1.5:1.6:1.8:1.9, respectively.

We focused on the CheY/CheZ FRET pair, because it provides a measure of the activity of the receptor complex, i.e., of the CheA kinase. The rate of transfer of phosphate from CheA~P to CheY is much faster than the rate of transfer of phosphate from ATP to CheA; therefore, the rate of formation of CheY~P is proportional to the concentration of the active receptor complex (for kinetic parameters, see ref. 26). The rate of hydrolysis of CheY~P catalyzed by CheZ is much faster than the uncatalyzed rate; therefore, the rate of hydrolysis of CheY~P is proportional to the concentration of the CheY~P/CheZ complex. At steady state, the rates of phosphorylation and hydrolysis are equal, so the activity of the receptor complex is proportional to the concentration of the CheY~P/CheZ complex, which is what FRET measures. On the time scale that we are working, the system remains near steady state, because the initial response is relatively fast and the rate of receptor modification is relatively slow.

We stimulated wild-type and mutant cells with steps of MeAsp across a range of concentrations and plotted the relative amplitudes of the initial response (Fig. 2). The wild-type response could be fit by a multisite Hill model with a single apparent K_D and little cooperativity. The apparent K_D was surprisingly small, only 2.6 μM, whereas the K_D measured by recovery time (27) or capillary assay (28) is 160 μM. However, in the latter assays, cells have time to adapt. Similar results were obtained with a CheY/FliM FRET pair (not shown), and the apparent K_D increased only about 2-fold in a *cheZ* background, confirming that CheZ does not play a significant role in signal amplification (29).

Mutants defective in methylation and/or demethylation showed a wide range of sensitivities, with K_D values ranging through 4 orders of magnitude (Fig. 2). Two K_Ds were apparent for *cheRcheB* strains, with values that depended on levels of Tar receptor modification. All the data could be fit by a multisite Hill model with little cooperativity. The K_D for the *cheR* strain was similar to that for the wild type, whereas the other values were much larger, on the order of 0.1 and 80 mM. The *cheRcheB* strains used here were *tap* mutants (Tap is a receptor of low abundance that interacts with dipeptide-binding proteins), so we compared QEQE *tap* and QEQE *tap*$^+$ strains and found their response curves to be the same (data not shown). *cheRcheB* cells lacking Tar still showed a response at the higher K_D, whereas *cheRcheB* cells lacking Tsr showed a response at a single K_D closer to that of the wild type (data not shown). In *cheRcheB* strains, the smaller K_D shifted upward at higher levels of modification (Fig. 2), as observed *in vitro* (12, 13, 30), whereas the larger K_D remained the same, as expected for binding to Tsr, which is in the same modification state (QEQE) in all of the *cheRcheB* strains. Thus, MeAsp apparently signals through both major chemoreceptors, and interactions between these chemoreceptors might be important.

The appearance of two apparent dissociation constants was not an artifact of a MeAsp contaminant, because responses of *cheRcheB* cells to synthetic L-aspartate also showed two K_D values: 3.5 ± 0.5 μM and 55 ± 5 mM for the EEEE strain, and 7.1 ± 1.7 μM and 62 ± 6 mM for the QEQE strain (data not shown). The smaller K_D values are the same as the dissociation constants for the EEEE and QEQE receptors measured *in vitro* (12). Thus, as suggested by others (29, 31), the responses of *cheRcheB* mutants reveal the true dissociation constants.

We also studied chemotactic responses of wild-type cells at different ambient concentrations of attractant (Fig. 3). Sensitivity to further addition (or removal) of attractant decreased with ambient concentration (Fig. 3*A*). At any given ambient, the K_D for removal of attractant was always two or three times higher than the K_D for addition. From the curves for addition we read off the fractional change in kinase activity, $1 - N/N_{pre}$, expected for a fractional change in concentration of 0.1 or 0.2, and plotted the ratio of output to input (the sensitivity) as a function of ambient concentration, as shown by the solid lines in Fig. 3*B*. We repeated this procedure for the fractional change in kinase activity found for *cheRcheB* cells (Fig. 2), as shown by the dashed lines in Fig. 3*B*. In this case, differences for fractional changes in concentration of 0.1 or 0.2 were so small that only one set of curves is shown, differing only in the extent of receptor modification. The two families of curves are offset by a fixed ratio on the order of 35 throughout the full range of ambient concentrations. The simplest explanation for this result is that, in wild-type cells, the fractional change in kinase activity is 35 times larger than the fractional change in receptor occupancy, assuming that the receptors function with the K_D values determined for *cheRcheB* mutants, as justified above. The amplification factor, computed from the points on the QEQE curve, averages 37 ± 9. A more precise estimate would require detailed knowledge of changes in receptor modification, e.g., use of curves for more highly modified receptor at higher ambient concentrations.

This interpretation is refined in Fig. 3*C*, which shows that families of curves of the sort shown in Fig. 3*A* collapse onto a single curve if the FRET response is plotted as a function of the fractional change in receptor occupancy, again, assuming K_D values determined for *cheRcheB* mutants. Fig. 3*C Inset* shows the same data plotted on a linear scale for small changes in receptor

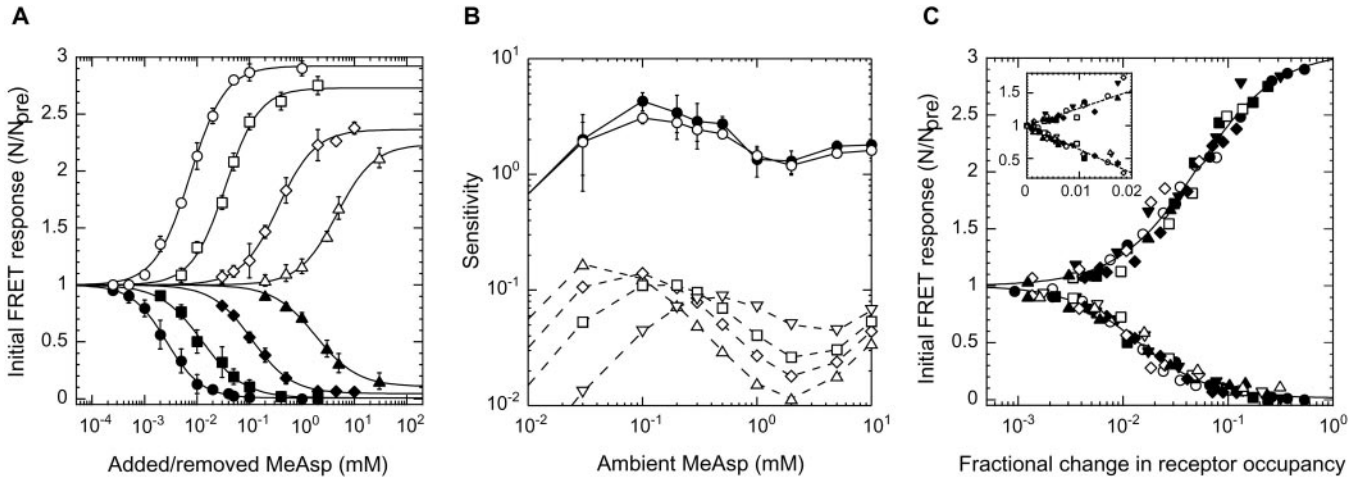

Fig. 3. Response of wild-type cells to steps of MeAsp at different ambient concentrations, measured with the CheY/CheZ FRET pair. (*A*) Initial response amplitudes as a function of the magnitude of the step change in concentration of MeAsp after complete adaptation to ambient concentrations 0 (●), 0.1 (■), 0.5 (◆), and 5 mM (▲). Additional MeAsp was added (closed symbols) and then removed (open symbols) in a sequence of steps of increasing size (as in Fig. 2). Hill coefficients were 1.2 ± 0.1. (*B*) Dependence of response sensitivity on changes in the concentration of MeAsp of 10% (●) or 20% (○), as a function of the ambient concentration (solid lines, *Upper*). Sensitivity is defined as the fractional change in FRET, $(1 - N/N_{pre})$, divided by the fractional change in concentration. Also shown is the sensitivity calculated for *cheRcheB* cells with EEEE (△), QEEE (◇), QEQE (□), or QEQQ (▽) receptors, using the fits to the response curves of Fig. 2 (dashed lines, *Lower*). (*C*) Data from experiments of the sort shown in *A* plotted as a function of fractional change in receptor occupancy. All the points shown represent measured values of N/N_{pre}. The corresponding change in receptor occupancy was computed by using the fit to the response curve for the QEQE receptor, except at 0 ambient, where a 0.5:0.5 combination of EEEE and QEEE receptors was assumed. The smooth curves are fits to the pooled data of a multisite Hill model: for addition of attractant, apparent K_D 0.014 ± 0.001, Hill coefficient 1.28 ± 0.05; for removal of attractant, apparent K_D 0.050 ± 0.004, Hill coefficient 1.14 ± 0.06. (*Inset*) The same data for small changes in receptor occupancy, plotted on a linear scale. The smooth curves are linear fits (slopes −36 ± 1 and 27 ± 2, respectively). The different ambient concentrations were (in millimolar) 0 (●), 0.03 (▼), 0.1 (■), 0.2 (▽), 0.3 (□), 0.5 (◆), 1 (○), 2 (◇), 5 (▲), and 10 (△).

occupancy (0–0.02). The response was linear throughout this regime, with a slope for addition of attractant –36 ± 1 and for removal of attractant 27 ± 2. Amplification has been noted in experiments with swimming cells, but with a lower magnitude and a logarithmic dependence (29), which Fig. 3*C* shows might be expected for large changes in receptor occupancy.

Discussion

The changes in receptor occupancy encountered by bacteria swimming in spatial gradients (e.g., near the mouth of a capillary tube in the capillary assay) are very small. For example, in the tracking experiments (1), cells about 0.6 mm from the tip of a capillary tube containing 1 mM aspartate moved in a gradient of steepness 0.02 μM/μm at a mean concentration of about 8 μM. A 10-μm run straight up such a gradient would change the concentration from 8 to 8.2 μM, i.e., by 2.5%. Assuming K_D values for aspartate of 7.1 μM and 62 mM (see above), this step gives a fractional change in receptor occupancy of about 0.003, well within the linear range of Fig. 3*C*. Runs up the gradient increased in length by about 30%, on average (1). When tethered cells were exposed to a step in the concentration of MeAsp from 160 to 163 μM, the rotational bias changed by 0.23 (19). By using our K_D values, the corresponding change in receptor occupancy was 0.002. Fig. 3*C Inset* shows that the fractional change in kinase activity expected for this change in receptor occupancy is about 0.07. So, if the concentration of CheY~P in a fully adapted cell is near the midpoint of the motors' ultrasensitive response curve (18), say 3.1 μM, that concentration would fall to about 2.9 μM, and the rotational bias would decrease by about 0.17. So, the amplification factor of 36 is close to the value required to explain the paradox of high chemotactic gain.

That responses are proportional to changes in receptor occupancy has seemed clear for a long time (27, 28). What is new and gratifying is the large size of the constant of proportionality. How does this amplification come about? Given the high sensitivity (albeit low amplitude) of the response in *cheR* cells (Fig. 2) compared with the low sensitivity in *cheRcheB* and *cheB* cells, our results suggest that amplification is CheB-dependent. A model in which CheB plays a pivotal role in amplification has been proposed by Barkai *et al.* (31). An alternative is amplification by receptor–receptor interaction (32); however, this hypothesis, as currently formulated, does not predict uniform amplification across a wide range of ambient concentrations. Before we reach a firm conclusion, we need to learn more about mutants defective in CheB phosphorylation and about the interdependence of activities of receptors of different types.

We thank Dennis Bray and Sandy Parkinson for their comments on the manuscript. This work was supported by a grant from the National Institutes of Health and by the Rowland Institute for Science.

1. Berg, H. C. & Brown, D. A. (1972) *Nature (London)* **239,** 500–504.
2. Falke, J. J., Bass, R. B., Butler, S. L., Chervitz, S. A. & Danielson, M. A. (1997) *Annu. Rev. Cell Dev. Biol.* **13,** 457–512.
3. Borkovich, K. A., Kaplan, N., Hess, J. F. & Simon, M. I. (1989) *Proc. Natl. Acad. Sci. USA* **86,** 1208–1212.
4. Welch, M., Oosawa, K., Aizawa, S.-I. & Eisenbach, M. (1993) *Proc. Natl. Acad. Sci. USA* **90,** 8787–8791.
5. Alon, U., Camarena, L., Surette, M. G., Aguera y Arcas, B., Liu, Y., Leibler, S. & Stock, J. B. (1998) *EMBO J.* **17,** 4238–4248.
6. Scharf, B. E., Fahrner, K. A., Turner, L. & Berg, H. C. (1998) *Proc. Natl. Acad. Sci. USA* **95,** 201–206.
7. Hess, F., Oosawa, K., Kaplan, N. & Simon, M. I. (1988) *Cell* **53,** 79–87.
8. Blat, Y. & Eisenbach, M. (1994) *Biochemistry* **33,** 902–906.
9. Borkovich, K. A. & Simon, M. I. (1990) *Cell* **63,** 1339–1348.
10. Springer, M. S., Goy, M. F. & Adler, J. (1979) *Nature (London)* **280,** 279–284.
11. Ninfa, E. G., Stock, A., Mowbray, S. & Stock, J. (1991) *J. Biol. Chem.* **266,** 9764–9770.
12. Borkovich, K. A., Alex, L. A. & Simon, M. I. (1992) *Proc. Natl. Acad. Sci. USA* **89,** 6756–6760.
13. Dunten, P. & Koshland, D. E., Jr. (1991) *J. Biol. Chem.* **266,** 1491–1495.
14. Herman, B. (1989) *Methods Cell Biol.* **30,** 219–243.
15. Miyawaki, A. & Tsien, R. Y. (2000) *Methods Enzymol.* **327,** 472–500.

16. Selvin, P. R. (2000) *Nat. Struct. Biol.* **7,** 730–734.
17. Wouters, F. S., Verveer, P. J. & Bastiaens, P. I. H. (2001) *Trends Cell Biol.* **11,** 203–211.
18. Cluzel, P., Surette, M. & Leibler, S. (2000) *Science* **287,** 1652–1655.
19. Segall, J. E., Block, S. M. & Berg, H. C. (1986) *Proc. Natl. Acad. Sci. USA* **83,** 8987–8991.
20. Sourjik, V. & Berg, H. C. (2000) *Mol. Microbiol.* **37,** 740–751.
21. Guzman, L.-M., Belin, D., Carson, M. J. & Beckwith, J. (1995) *J. Bacteriol.* **177,** 4121–4130.
22. Berg, H. C. & Block, S. M. (1984) *J. Gen. Microbiol.* **130,** 2915–2920.
23. Tokunaga, M., Kitamura, K., Saito, K., Iwane, A. H. & Yanagida, T. (1997) *Biochem. Biophys. Res. Commun.* **235,** 47–53.
24. Skerker, J. M. & Berg, H. C. (2001) *Proc. Natl. Acad. Sci. USA* **98,** 6901–6904. (First Published May 29, 2001; 10.1073/pnas.121171698)
25. Hill, A. V. (1913) *Biochem. J.* **7,** 471–480.
26. Morton-Firth, C. J., Shimizu, T. S. & Bray, D. (1999) *J. Mol. Biol.* **286,** 1059–1074.
27. Berg, H. C. & Tedesco, P. M. (1975) *Proc. Natl. Acad. Sci. USA* **72,** 3235–3239.
28. Mesibov, R., Ordal, G. W. & Adler, J. (1973) *J. Gen. Physiol.* **62,** 203–223.
29. Kim, C., Jackson, M., Lux, R. & Khan, S. (2001) *J. Mol. Biol.* **307,** 119–135.
30. Bornhorst, J. A. & Falke, J. J. (2000) *Biochemistry* **39,** 9486–9493.
31. Barkai, N., Alon, U. & Leibler, S. (2001) *C. R. Acad. Sci. Sér. IV* **2,** 871–877.
32. Duke, T. A. J. & Bray, D. (2001) *Proc. Natl. Acad. Sci. USA* **96,** 10104–10108.